with actionomycete, as were the following common microfungi: *Absidia* sp., *Ascobolus crenulatus*, *Aspergillus fumigatus*, *Coprinus patouillardii*, *Cryptococcus albidus*, *Drechslera biseptata*, *Exophiala spinifera*, *Fusarium oxysporum*, *Mucor pyriformis*, *Penicillium* sp., *Pythium aphanidermatum*, *Schizophyllum commune*, *Sordaria fimicola* and *Trichoderma* sp.

Each *Streptomyces*–fungal challenge was replicated three times and done on Czapek yeast autolysate agar. The actinomycete was inoculated on Petri dishes and grown to a diameter of ~1.5 cm; fungal strains were then point-inoculated near the edge of the culture. Challenges were monitored every two days and growth inhibition of tested fungi was scored as a reduction of growth rate as compared with growth of fungal cultures in the absence of the *Streptomyces*, or as complete suppression of growth. We assayed possible antibiotic production specific to the specialized parasite *Escovopsis* in the same way that we assayed antibiotic production specific to other potential contaminants, except that each challenge to *Escovopsis* was replicated five times. Four strains of *Escovopsis* isolated from the gardens of different *Acromyrmex octospinosus* colonies in Panama in 1997 were tested against *Streptomyces*. We also studied the production of antibiotics specific towards *Escovopsis* in other attine species, including *Cyphomyrmex longiscapus*, *Atta colombica* and *Atta cephalotes*. The presence of a zone of inhibition in bioassays indicates first, the production of diffusible metabolites by the actinomycete, and second, the susceptibility of the test fungus to these compounds. As inhibition is dose dependent, the detection of partial inhibition implies the existence of a dose that could impart complete inhibition.

Growth-promotion bioassays. Broth cultures of the attine fungus isolated from an *Apterostigma* colony were grown with extracts from the *Streptomyces* isolated from this species. Actinomycete extracts were obtained by growing *Streptomyces* in Czapek yeast autolysate broth for 2 weeks and then passing the broth through a low protein-binding, sterilizing filter unit (Millipore, Millex) to remove bacterial biomass. We replicated each bioassay five times and used 50 ml Czapek yeast autolysate broth per bioassay.

Received 20 November 1998; accepted 18 February 1999.

1. Weber, N. The fungus growing ants. *Science* **121,** 587–604 (1966).
2. Wilson, E. O. *The Insect Societies* (Belknap, Cambridge, Massachusetts, 1971).
3. Chapela, I. H., Rehner, S. A., Schultz, T. R. & Mueller, U. G. Evolutionary history of the symbiosis between fungus-growing ants and their fungi. *Science* **266,** 1691–1694 (1994).
4. Mueller, U. G., Rehner, S. A. & Schultz, T. R. The evolution of agriculture in ants. *Science* **281,** 2034–2038 (1998).
5. North, R. D., Jackson, C. W. & Howse, P. E. Evolutionary aspects of ant-fungus interactions in leaf-cutting ants. *Trends Ecol. Evol.* **12,** 386–389 (1997).
6. Currie, C. R., Mueller, U. G. & Malloch, D. The agricultural pathology of ant fungal gardens. *Proc. Natl Acad. Sci. USA* (submitted).
7. Wilson, E. O. in *Fire Ants and Leaf-cutting Ants.* (Westview, Builder, 1986).
8. Schultz, T. R. & Meier, R. A phylogenetic analysis of the fungus-growing ants (Hymenoptera: Formicidae: Attini) based on morphological characters on the larvae. *Syst. Entomol.* **20,** 337–370 (1995).
9. Hölldobler, B. & Wilson, E. O. *The Ants* (Belknap, Cambridge, Massachusetts, 1990).
10. Weber, N. A. *Gardening Ants: The Attines* (Am. Phil. Soc., Philadelphia, 1972).
11. Waksman, S. A. & Lechevalier, H. A. 1962. *The Actinomycetes, Vol. III. Antibiotics of Actinomycetes* (Williams & Wilkins, Baltimore, 1962).
12. Goodfellow, M. & Cross, T. *The Biology of Actinomycetes* (Academic, London, 1984).
13. Seifert, K. A., Samson, R. A. & Chapela, I. H. *Escovopsis aspergilloides*, a rediscovered hyphomycete from leaf-cutting ant nests. *Mycologia* **87,** 407–413 (1995).
14. Martin, M. M. & Martin, J. S. The biochemical basis for the symbiosis between the ant, *Atta colombica tonsiper*, and its food fungus. *J. Insect Physiol.* **16,** 109–119 (1970).
15. Hervey, A., Rogerson, C. T. & Leong, I. Studies on fungi cultivated by ants. *Brittonia* **29,** 226–236 (1978).
16. Cazin, J. Jr, Wiemer, D. F. & Howard, J. J. Isolation, growth characteristics, and long-term storage of fungi cultivated by attine ants. *Appl. Env. Microbiol.* **55,** 1346–1350 (1989).
17. Vining, L. C. Functions of secondary metabolites. *Annu. Rev. Microbiol.* **44,** 395–427 (1990).
18. Griffin, D. H. *Fungal Physiology* (Wiley-Liss, New York, 1994).
19. Eisner, T. Prospecting for nature's chemicals. *Iss. Sci. Tech.* **6,** 31–34 (1990).
20. Beattie, A. J. Discovering new biological resources—chance or reason. *Bioscience* **42,** 290–292 (1992).
21. Caporale, L. H. Chemical ecology: a view from the pharmaceutical industry. *Proc. Natl Acad. Sci. USA* **92,** 75–82 (1995).
22. Holt, J. G. *et al.* (eds) *Bergey's Manual of Determinative Microbiology* 9th edn. (Williams & Wilkings, Baltimore, 1994).
23. Wetterer, J. K., Schultz, T. R. & Meier, R. Phylogeny of fungus-growing ants (tribe Attini) based on mtDNA sequence and morphology. *Mol. Phylogenet. Evol.* **9,** 42–47 (1998).

Acknowledgements. This work was supported by Smithsonian and NSERC predoctoral awards (to C.R.C.) and an NSERC grant (to D.M.). C.R.C. thanks the Smithsonian Tropical Research Institute and ANAM of the Republic of Panama for assisting with the research and granting collecting permits, and U. G. Mueller for guidance, support and encouragement. We thank I. Ahmad, N. Alasti-Faridani, G. de Alba, S. Barrett, E. Bermingham, A. Caballero, J. Ceballo, S. Dalla Rosa, L. Ketch, M. Leone, G. Maggiori, S. Rand and M. Witkowska for logistical support; C. Ziegler for the photograph in Fig. 1; and K. Boomsma, J. Bot, R. Cocroft, G. Currie, J. Gloer, A. Herre, H. Herz, S. Rehner, T. Schultz, N. Straus, B. Wcislo and B. Wong for comments on this study and/or manuscript.

Correspondence and requests for materials should be addressed to C.R.C. (e-mail: currie@botany.utoronto.ca).

Relative reward preference in primate orbitofrontal cortex

Léon Tremblay* & Wolfram Schultz

Institute of Physiology and Program in Neuroscience, University of Fribourg, CH-1700 Fribourg, Switzerland

** Present address: INSERM Unit 289, Hôpital de la Salpetrière, 47 Boulevard de l'Hôpital, F-75651 Paris, France.*

The orbital part of prefrontal cortex appears to be crucially involved in the motivational control of goal-directed behaviour[1,2]. Patients with lesions of orbitofrontal cortex show impairments in making decisions about the expected outcome of actions[3]. Monkeys with orbitofrontal lesions respond abnormally to changes in reward expectations[4,5] and show altered reward preferences[6]. As rewards constitute basic goals of behaviour[7], we investigated here how neurons in the orbitofrontal cortex of monkeys process information about liquid and food rewards in a typical frontal task, spatial delayed responding[8]. The activity of orbitofrontal neurons increases in response to reward-predicting signals, during the expectation of rewards, and after the receipt of rewards. Neurons discriminate between different rewards, mainly irrespective of the spatial and visual features of reward-predicting stimuli and behavioural reactions. Most reward discriminations reflect the animals' relative preference among the available rewards, as expressed by their choice behaviour, rather than physical reward properties. Thus, neurons in the orbitofrontal cortex appear to process the motivational value of rewarding outcomes of voluntary action.

Neurophysiological studies of behaving monkeys and rats show that neurons in the six-layered parts of orbitofrontal cortex process motivating events, discriminate between appetitive and averse conditioned stimuli[9] and are active during the expectation of outcomes[10]. Some orbitofrontal neurons may code the value of reward objects in losing their responses when animals become satiated on particular food items[11]. Neurons in more caudal, three- and four-layered orbitofrontal regions process gustatory and olfactory information[12–14].

We investigated the motivational properties of orbitofrontal neurons in macaque monkeys during a spatial delayed-response task (Fig. 1). The position of a briefly presented instruction picture indicated the target of an arm movement, and its visual features predicted specifically which of two liquid or food rewards would be delivered for correct performance at the end of the trial. A subsequent uniform trigger stimulus provoked the movement to the remembered target. The reward was delivered after a brief delay during which the animal could expect the reward. Reaction times

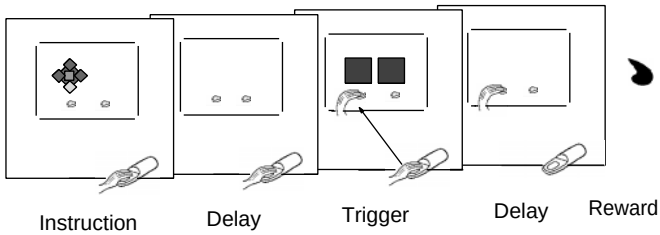

Figure 1 Spatial delayed-response task. An initial instruction picture indicates the left or right target of movement and the liquid or food reward that will be delivered at the end of the trial. Following a brief delay, two identical squares appear and the monkey moves its hand from the resting key to the left or right target lever indicated by the instruction. Correct performance is rewarded after a brief delay with a drop of liquid or a morsel of food.

differed significantly between trials with different rewards, indicating that monkeys had established reward expectations[15,16].

Neurons in six-layered parts of orbitofrontal areas 11 and 14 and rostral area 13 (Fig. 2) showed three principal types of activation, namely responses to instructions (15% of 1,095 tested neurons in liquid-rewarded trials, 15% of 329 neurons in food-rewarded trials), responses following reward (8% in liquid, 18% in food trials), and sustained activations preceding reward (9% in liquid, 19% in food trials). The pre-reward activations began several seconds before the reward, increased slowly and subsided <1 s after reward delivery, apparently reflecting the upcoming reward rather than preceding events. They were unrelated to arm movements, as they also occurred in non-movement trials of a delayed go/no-go task with similar temporal structure (87% of 47 neurons; L.T. and W.S., manuscript in preparation). Similar pre-reward activations occur in basal ganglia neurons[16–18] and probably reflect the expectation of reward. In contrast, statistically significant sustained activations during the entire instruction–trigger delay were only found in two neurons, although they are frequent in dorsolateral prefrontal cortex[19–21]. Thus, most orbitofrontal neurons modulated here were activated in response to reward-related events.

All three principal types of orbitofrontal activation discriminated between different liquid rewards and between different food rewards (Fig. 3). Activations occurred only, or were significantly

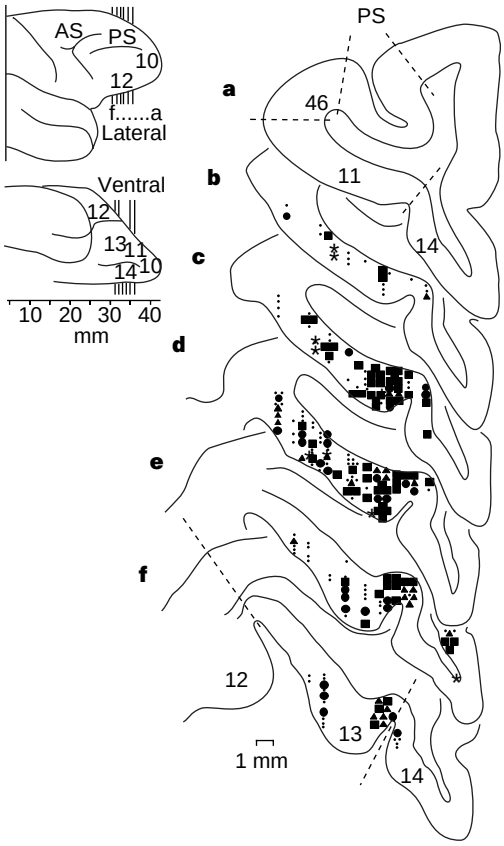

Figure 2 Positions of orbitofrontal neurons activated in liquid-reward trials. Vertical lines in the left-hand diagrams indicate rostrocaudal levels of electrode penetrations corresponding to frontal sections a–f of the right-hand diagram. Right, each symbol shows the position of a single neuron. Filled squares, neurons responding to instructions; filled circles, neurons activated pre-reward or post-reward; filled triangles, neurons responding to instructions and activated pre-or post-reward; stars, neurons with spatial relationships; small dots, activations unselective for reward, spatial position or instruction pictures. Numbers refer to architectonic areas. Area 12 was not studied. AS, arcuate sulcus; PS, principal sulcus.

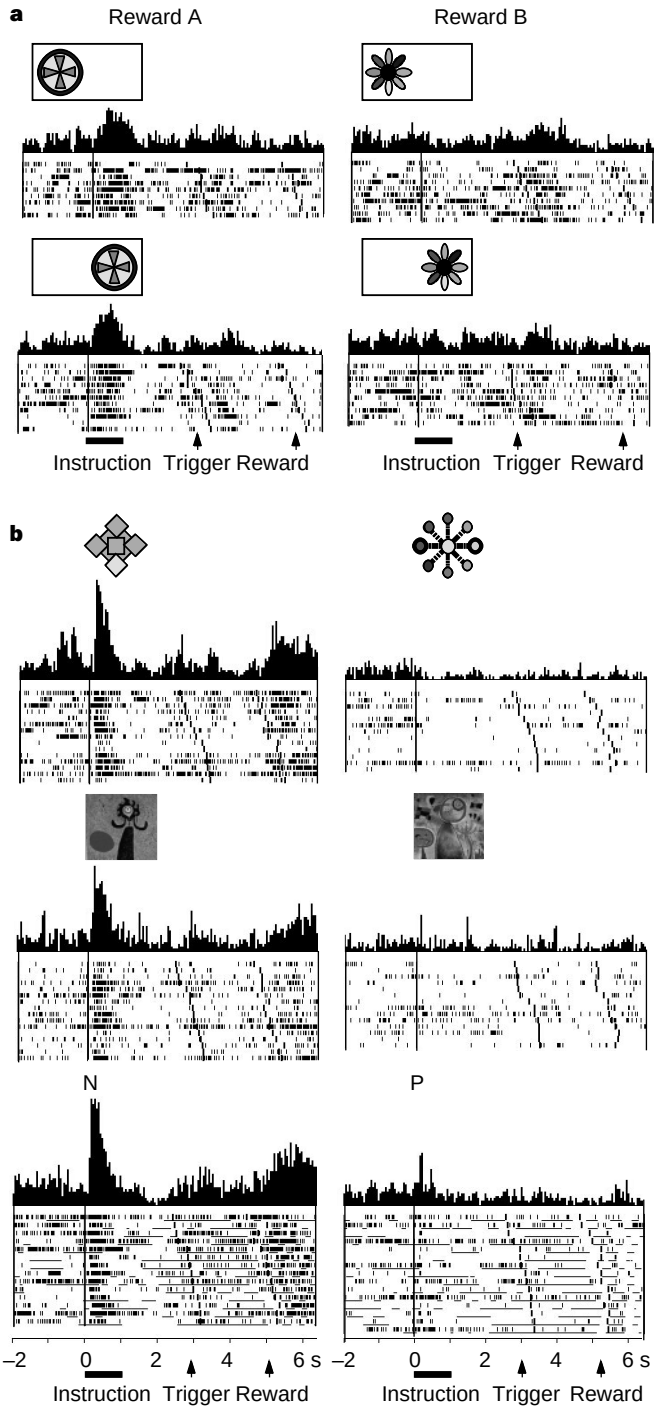

Figure 3 Reward rather than spatial or object processing in orbitofrontal neurons. **a**, The response to instructions shown by a single orbitofrontal neuron that discriminates between liquid rewards but not between left and right instruction positions. The insets above the histograms show the instruction pictures used, at left or right positions. Reward A, grenadine juice; reward B, apple juice. Raster dots denote neuronal impulses aligned to instruction onset. Each line shows one trial. Use of the two rewards and positions were alternated randomly between trials; trials are separated for analysis. The original trial sequence is shown from top to bottom. **b**, Response to instructions shown by a single orbitofrontal neuron that discriminates between liquid rewards but not between visual instruction features. Instruction responses differed insignificantly between the three different instructions predicting reward A (grape juice). Reward B was orange juice. The three instruction sets were tested in separate trial blocks and are shown above the corresponding neuronal data. Thin horizontal lines in the bottom blocks indicate licking periods. This neuron also responded following delivery of reward A. N, P represent the pictures used.

higher, for one reward compared with the other rewards in 69% of 218 instruction responses, 52% of 146 reward responses and 41% of 160 pre-reward activations. These differences were unrelated to eye or licking movements before or after reward delivery; these movements varied inconspicuously between the two rewards referred to in Fig. 3b, bottom. Only 3% of 218 instruction responses discriminated between left and right targets of movement, and none of the 50 neurons tested with several instruction sets showed significantly different responses to different instructions indicating the same reward. Thus orbitofrontal neurons reflected the predicted rewards much better than they reflected the spatial or visual features of the instructions in the present task situation.

When subjects have a choice between different rewards, they may select some rewards more frequently than others. However, the preferences expressed by overt choice behaviour are relative and depend on the available alternatives. A reward that is chosen more frequently in the presence of some rewards may be instantly neglected when other, more appetizing rewards become available. Apparently, motivational values, unlike physical properties, are not fixed to individual rewards. The question arose to what extent the prominent reward relationships of orbitofrontal neurons might reflect the relative motivational values of rewards expressed by choice behaviour. This relates to the observation that monkeys with ventromedial prefrontal lesions show abnormal reward preferences[6].

We obtained behavioural evidence for relative reward preference in a choice version of the task used above. Two instruction pictures, instead of one, were shown simultaneously above the left and right levers, respectively. Each picture was associated with a different reward. Following the trigger stimulus, animals chose one of the rewards by touching the corresponding lever. We used three food rewards (A–C) but presented only two of them in a given trial block (A and B, B and C, or A and C). Animals showed clear preferences in every comparison, choosing rewards A over B, B over C, and A over C in 90–100% of trials, independently of the side of the touched lever. Thus reward B was chosen less frequently when reward A was available, but more frequently when reward C was available. The preference for reward B seemed to be relative and depended on the reward with which it was being compared.

We studied orbitofrontal neurons during the performance in the standard delay task described above, in which animals were presented with a single instruction picture for a single, preferred or non-preferred, reward. Two rewards alternated randomly in each trial block, and usually all three combinations of reward pairs were tested (A and B, B and C, and A and C in separate blocks). The relative preference of the animal was checked in separate choice trials before or after each recording block. The activity of 40 of 65 reward-discriminating orbitofrontal neurons indeed depended on the combination in which a particular reward occurred. The neuron of Fig. 4 showed significantly higher activation preceding reward A (preferred) as compared with reward B (non-preferred) (Fig. 4, top). When reward B was compared with reward C in a different trial block (Fig. 4, bottom), the same neuron was activated significantly more preceding reward B (now preferred) than reward C (non-preferred). Neuronal activations preceding reward B occurred only when this reward was the preferred one (Fig. 4, centre, compare top and bottom panels). Thus, this orbitofrontal neuron was activated by the reward that was relatively more preferred than the available alternative. Comparable results were seen with reward-predicting instruction responses and with responses following the reward (total of 27 neurons). The reverse was observed with 13 of the 40 neurons, which showed higher activations in response to whichever reward was less preferred than the available alternative in the A and B, B and C scheme. Neurons with activity reflecting relatively higher or lower reward preference were located in posteriomedial area 11, close to area 14 (sections c–e of Fig. 2). Thus, the reward discrimination occurred in some orbitofrontal neurons on the basis of relative preference rather than physical properties.

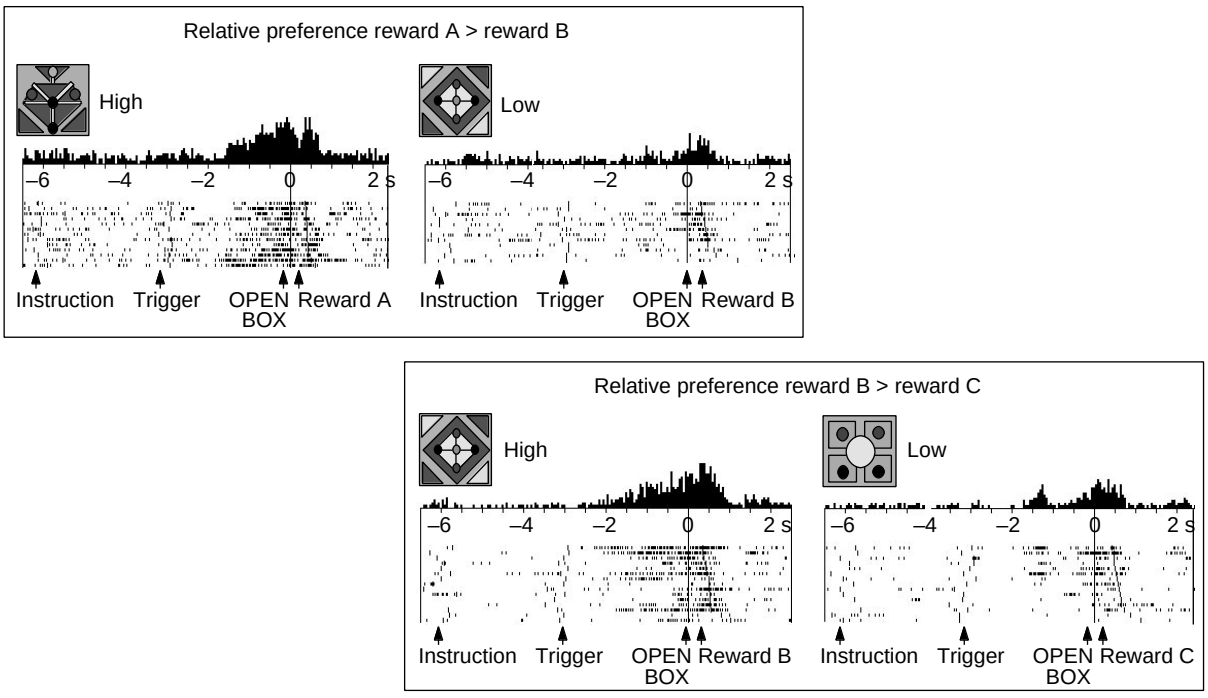

Figure 4 Coding of relative reward preference in an orbitofrontal neuron. Neuronal activity increased during the expectation period preceding the relatively more preferred food reward (raisin in top panel, apple in bottom panel). Although reward B (apple) was physically identical in the top and bottom panels, its motivational value was relative and differed according to the other available reward (its motivational value was low in the top panel and high in the bottom panel), as expressed by the animal's choice behaviour assessed in separate trials. Different combinations of reward were used in the two trial blocks (A, raisin; B, apple; C, cereal). Each reward was specifically predicted by an instruction picture, which is shown above the histograms. Lever touch following the movement-trigger stimulus induced, 2 s later, the opening of a food box from which the animal collected the reward.

Nearly all task-related activations in the remaining 25 of the 65 neurons occurred in response to either the most preferred (A) or the least preferred (C) of the three food rewards. These activations were independent of the combination of rewards. Only a single neuron responded to the instruction for the intermediately preferred reward, B, in all comparisons.

These results show that some orbitofrontal neurons process specific aspects of motivational information. They discriminate well between different rewards, and many discriminations appear to be based on the relative preference for different rewards exhibited by animals in overt choice behaviour. The activity of these orbitofrontal neurons does not appear to code the fixed physical properties of rewards, but rather reflects the motivational value of one reward relative to another, as expressed by the behavioural preference. Just as each reward can have a higher or lower motivational value relative to the reward with which it is compared, orbitofrontal neurons can be more or less activated by one reward, depending on which alternative reward is available.

Primates are able to consume hundreds of different reward objects, but only a few objects are available at any given time. The coding of relative preferences among the available rewards would allow orbitofrontal neurons to specify motivational goals of behaviour in far more situations than would be allowed by coding of the physical properties of individual rewards.

Many neurons in both the dorsolateral and ventrolateral prefrontal cortex process spatial positions and/or visual features of environmental objects[20–24]. These functions may be derived from inputs from posterior parietal cortex and inferotemporal cortex[25,26]. The orbitofrontal neurons studied here seem to process basic motivational aspects of environmental events that determine the probability and intensity of goal-directed behaviour. These activities may result from trans-synaptic inputs from the striatum, which shows prominent relationships to reward expectation[16–18], and from inputs from the amygdala and rostral and medial temporal lobe[27,28]. Interestingly, the delivery of reward also produces responses in ventrolateral prefrontal neurons[29], and expected rewards influence spatial delay activity of dorsolateral prefrontal neurons[30]. □

Methods

Behavioural task. Two *Macaca fascicularis* monkeys performed a spatial delayed-response task for liquid or food reward. The monkeys kept their right hands relaxed on an unmovable resting key. The monkeys faced a 13-inch computer screen positioned behind a transparent plastic wall in which two small levers were mounted to the left and right of the midline. To start each trial, a colour instruction picture (13° × 13°) appeared for 1 s on a computer screen above the left or right lever (Fig. 1). After a randomly varied delay of 2.5–3.5 s, two identical red squares appeared simultaneously as movement-trigger stimuli at the left and right positions of the instruction. The moderately fluid-or food-deprived animal released a key, touched the lever at the position previously indicated by the instruction and received a liquid or food reward for correct performance. Both squares disappeared upon lever touch.

Liquid rewards (0.15 ml) were dispensed 1.5 or 2.0 s after lever touch by a computer-controlled liquid valve from a spout at the animal's mouth. Liquids were grenadine and apple juice for one monkey, and orange and grape juice for the second monkey. Food rewards were presented 2.0 s after lever touch in a box located to the right of the computer screen following computer-controlled opening of its door (40 mm × 40 mm frontal opening). Foods were raisins (most preferred), small apple morsels (intermediately preferred) and sugar–honey cereal (least preferred). Each reward was indicated at trial onset by a specific instruction picture. To assess the influence of visual features on neuronal responses, we used five different pairs of instruction pictures in liquid trials (four of which are shown in Fig. 3) and one set of three pictures in food trials (Fig. 4). Only two instruction pictures, with their associated two liquid or two food rewards, were presented in a given block of trials.

Reward preferences were assessed in separate blocks of choice trials before or after recording from each neuron. Two different instructions for two rewards were shown simultaneously at randomly alternating left and right target positions, allowing the animal to touch the lever of its choice following the trigger stimulus. All rewards were used in combinations in which animals showed reliable and persistent preferences. Thus, each pair of instruction stimuli contained one picture associated with a preferred reward and one with a non-preferred reward. Rewards and target positions alternated randomly, with a maximum of three consecutive identical trials. Trials lasted 12–14 s; intertrial intervals were 4–6 s.

Electrophysiological recording. The activity of single neurons in the left orbitofrontal cortex was recorded extracellularly with movable microlectrodes for 20–60 min in the two monkeys, using standard electrophysiological techniques. During neuronal recordings, arm-muscle activity, mouth-muscle activity and eye movements were monitored through chronically implanted electrodes, and licking movements were monitored with an infrared-light barrier interrupted by the animal's tongue. Following analog-to-digital conversion, muscle activity and eye movements were exhibited in single-trial or averaged mode in reference to individual task events. Task-related neuronal changes were assessed with the sliding-window procedure based on the one-tailed Wilcoxon test ($P < 0.01$)[16,18]. Task-related activations were considered only from neurons tested in at least ten trials in a given situation and showing statistically significant activity increases in relation to at least one task event, compared with the spontaneous activity before the first task event. Task-related changes in individual neurons in response to first, different rewards, second, left and right targets, and third, corresponding pictures of different instruction sets were compared using the two-tailed Mann–Whitney *U*-test ($P < 0.05$), on impulse counts in single trials. Reaction times (from trigger stimulus onset to key release) in response to different rewards were compared using the two-tailed Mann–Whitney *U*-test ($P < 0.002$). Recording sites were marked with small electrolytic lesions and reconstructed from 40-μm-thick cresyl-violet-stained coronal sections of paraformaldehyde-perfused brains. Experimental protocols conformed to the Swiss Animal Protection Law and were supervised by the Fribourg Cantonal Veterinary Office.

Received 2 December 1998; accepted 10 February 1999.

1. Damasio, A R. *Descartes Error* (Putnam, New York, 1994).
2. Rolls, E. T. The orbitofrontal cortex. *Phil. Trans. R. Soc. Lond. B* **351,** 1433–1444 (1996).
3. Bechara, A., Damasio, H., Tranel, D. & Anderson, S. W. Dissociation of working memory from decision making within the human prefrontal cortex. *J. Neurosci.* **18,** 428–437 (1998).
4. Iversen, S. D. & Mishkin, M. Preservative interference in monkeys following selective lesions of the inferior prefrontal convexity. *Exp. Brain Res.* **11,** 376–386 (1970).
5. Dias, R., Robbins, T. W. & Roberts, A. C. Dissociation in prefrontal cortex of affective and attentional shifts. *Nature* **380,** 69–72 (1996).
6. Baylis, L. L. & Gaffan, D. Amygdalectomy and ventromedial prefrontal ablation produce similar deficits in food choice and in simple object discrimination learning for an unseen reward. *Exp. Brain Res.* **86,** 617–622 (1991).
7. Dickinson, A. & Balleine, B. Motivational control of goal-directed action. *Anim. Learn. Behav.* **22,** 1–18 (1994).
8. Jacobsen, C. F. & Nissen, H. W. Studies of cerebral function in primates: IV. The effects of frontal lobe lesions on the delayed alternation habit in monkeys. *J. Comp. Physiol. Psychol.* **23,** 101–112 (1937).
9. Thorpe, S. J., Rolls, E. T. & Maddison, S. The orbitofrontal cortex: neuronal activity in the behaving monkey. *Exp. Brain Res.* **49,** 93–115 (1983).
10. Schoenbaum, G., Chiba, A. A. & Gallagher, M. Orbitofrontal cortex and basolateral amygdala encode expected outcome during learning. *Nature Neurosci.* **1,** 155–159 (1998).
11. Critchley, H. G. & Rolls, E. T. Hunger and satiety modify the responses of olfactory and visual neurons in the primate orbitofrontal cortex. *J. Neurophysiol.* **75,** 1673–1686 (1996).
12. Critchley, H. G. & Rolls, E. T. Olfactory neuronal responses in the primate orbitofrontal cortex: analysis in an olfactory discrimination task. *J. Neurophysiol.* **75,** 1659–1672 (1996).
13. Schoenbaum, G. & Eichenbaum, H. Information coding in the rodent prefrontal cortex. I. Single-neuron activity in orbitofrontal cortex compared with that in pyriform cortex. *J. Neurophysiol.* **74,** 733–750 (1995).
14. Rolls, E. T., Critchley, H. D., Mason, R. & Wakeman, E. A. Orbitofrontal cortex neurons: role in olfactory and visual association learning. *J. Neurophysiol.* **75,** 1970–1981 (1996).
15. Tinklepaugh, O. L. An experimental study of representation factors in monkeys. *J. Comp. Psychol.* **8,** 197–236 (1928).
16. Hollerman, J. R., Tremblay, L. & Schultz, W. Influence of reward expectation on behavior-related neuronal activity in primate striatum. *J. Neurophysiol.* **80,** 947–963 (1998).
17. Hikosaka, O., Sakamoto, M. & Usui, S. Functional properties of monkey caudate neurons. III. Activities related to expectation of target and reward. *J. Neurophysiol.* **61,** 814–832 (1989).
18. Schultz, W., Apicella, P., Scarnati, E. & Ljungberg, T. Neuronal activity in monkey ventral striatum related to the expectation of reward. *J. Neurosci.* **12,** 4595–4610 (1992).
19. Fuster, J. M. & Alexander, G. E. Neuron activity related to short-term memory. *Science* **173,** 652–654 (1971).
20. Kubota, K. & Niki, H. Prefrontal cortical unit activity and delayed alternation performance in monkeys. *J. Neurophysiol.* **34,** 337–347 (1971).
21. Funahashi, S., Chafee, M. V. & Goldman-Rakic, P. S. Prefrontal neuronal activity in rhesus monkeys performing a delayed anti-saccade task. *Nature* **365,** 753–756 (1993).
22. Wilson, F. A. W., O'Scalaidhe, S. P. & Goldman-Rakic, P. S. Dissociation of object and spatial processing domains in primate prefrontal cortex. *Science* **260,** 1955–1958 (1993).
23. Rao, S. C., Rainer, G. & Miller, E. K. Integration of what and where in the primate prefrontal cortex. *Science* **276,** 821–824 (1997).
24. Miller, E. K., Erickson, C. A. & Desimone, R. Neural mechanisms of visual working memory in prefrontal cortex of the monkey. *J. Neurosci.* **16,** 5154–5167 (1996).

25. Petrides, M. & Pandya, D. N. Association fiber pathways to the frontal cortex from the superior temporal region in the rhesus monkey. *J. Comp. Neurol.* **273,** 52–66 (1988).
26. Pandya, D. N. & Yeterian, E. H. Comparison of prefrontal architectures and connections. *Phil. Trans. R. Soc. Lond. B* **351,** 1423–1432 (1996).
27. Barbas, H. Anatomic organization of basoventral and mediodorsal visual recipient prefrontal regions in the rhesus monkey. *J. Comp. Neurol.* **276,** 313–342 (1988).
28. Carmichael, S. T. & Price, J. L. Limbic connections of the orbital and medial prefrontal cortex in macaque monkeys. *J. Comp. Neurol.* **363,** 615–641 (1995).
29. Rosenkilde, C. E., Bauer, R. H. & Fuster, J. M. Single cell activity in ventral prefrontal cortex of behaving monkeys. *Brain Res.* **209,** 375–394 (1981).
30. Watanabe, M. Reward expectancy in primate prefrontal neurons. *Nature* **382,** 629–632 (1996).

Acknowledgements. We thank B. Aebischer, J. Corpataux, A. Gaillard, A. Pisani, A. Schwarz and F. Tinguely for technical assistance. The study was supported by the Swiss NSF (W.S.) and the Fondation pour la Recherche Scientifique de Quebec (L.T.).

Correspondence and requests for materials should be addressed to W.S. (e-mail: Wolfram.Schultz@unifr.ch).

p63 is a *p53* homologue required for limb and epidermal morphogenesis

Alea A. Mills*†, Binhai Zheng†, Xiao-Jing Wang‡§, Hannes Vogel‖, Dennis R. Roop‡§ & Allan Bradley*†

** Howard Hughes Medical Institute, and † Departments of Molecular and Human Genetics, ‡ Cell Biology and § Dermatology, Baylor College of Medicine, One Baylor Plaza, Houston, Texas 77030, USA*
‖ Department of Pathology, Texas Childrens Hospital, Houston, Texas 77030, USA

The p53 tumour suppressor is a transcription factor that regulates the progression of the cell through its cycle and cell death (apoptosis) in response to environmental stimuli such as DNA damage and hypoxia[1,2]. Even though p53 modulates these critical cellular processes, mice that lack p53 are developmentally normal[3], suggesting that p53-related proteins might compensate for the functions of p53 during embryogenesis. Two *p53* homologues, *p63* and *p73*, are known[4,5] and here we describe the function of p63 *in vivo*. Mice lacking p63 are born alive but have striking developmental defects. Their limbs are absent or truncated, defects that are caused by a failure of the apical ectodermal ridge to differentiate. The skin of p63-deficient mice does not progress past an early developmental stage: it lacks stratification and does not express differentiation markers. Structures dependent upon epidermal–mesenchymal interactions during embryonic development, such as hair follicles, teeth and mammary glands, are absent in p63-deficient mice. Thus, in contrast to p53, p63 is essential for several aspects of ectodermal differentiation during embryogenesis.

Two *p53*-related genes, human *p73* and rat *Ket*, have been described[4,5]. We cloned a mouse *p53* homologue referred to here as *p63*, using a polymerase chain reaction strategy designed to identify genes that contain homology to the highly conserved DNA-binding domain of *p53*. Sequence analysis indicates that this gene contains significant homology to *p53*, human *p73* and rat *Ket*. *p63* was mapped to mouse chromosome 16 between *D16Mit1* and *D16Mit3* (data not shown), which indicated that *p63* was not the mouse homologue of human *p73*. Complementary DNAs encoding the human homologue of *Ket* have recently been described and designated as *p40* (ref. 6), *p51* (ref. 7), and *p63* (ref. 8). Sequence alignments of rat *Ket*, mouse *p63* and human *p63* indicate that these genes are true homologues (data not shown).

Expression of *p63* was examined using *in situ* and northern-blot hybridization. *p63* is expressed as early as embryonic day 9.5 (E9.5) within the oral ectoderm, limb buds and tail bud region (see below). At later stages of gestation, *p63* is expressed primarily within the ectoderm; expression is evident within the basal region of the interfollicular epidermis of the skin and within the outer root-sheath of hair follicles (data not shown). In adult mice, northern-blot analysis indicates that *p63* is expressed in skin, tongue, tail and skeletal muscle (data not shown).

To assess the function of p63 during embryogenesis, we mutated the *p63* gene using embryonic stem (ES) cell technology. Two different targeting vectors, pTV6H(90) and pTV12E(60), were identified that integrate into different regions of the *p63* locus, and these were used to generate different mutant alleles of the *p63* gene (Fig. 1a). These vectors were isolated from a library of pre-prepared vectors[31] which use the gap-repair mechanism in their gene-targeting reactions[9]; an internal fragment was deleted from the region of homology for use as a diagnostic probe to detect gene targeting. The pTV6H(90) vector generates a recombinant allele that is predicted to truncate the transcript within exon 6 and which, if translated, would create a protein with a non-functional DNA-binding domain; this allele is referred to as $p63^{Brdm1}$. The pTV12E(60) vector generates a recombinant allele, $p63^{Brdm2}$, that truncates the messenger RNA at exon 10: this transcript (if translated) would yield a protein containing an intact DNA-binding domain, but not the highly conserved 3′ region of the p63 protein. Targeted ES cell clones were identified and chimaeras were generated by blastocyst microinjection. Multiple independent ES clones representing each class of recombinant allele transmitted their mutant *p63* alleles into the germ line.

F_1(129/C57B6) heterozygous mutant mice were intercrossed, ~25% of the pups from these matings were born with a shiny, transparent skin (Fig. 2a). These pups had abnormal facies, truncations of the forelimbs, and were without hindlimbs. Determination of the genotype of mice with this phenotype showed that they were exclusively homozygous mutants (Fig. 1b). Northern-blot analysis indicated that *p63*-homozygous mutant animals do not express the *p63* transcript (Fig. 1c), so these are likely to be null alleles. Independent clones representing the two different mutant alleles $p63^{Brdm1}$ and $p63^{Brdm2}$ produced an identical phenotype (Fig. 2a) and therefore were not distinguished in subsequent experiments.

Although p63-deficient animals were viable at birth, they died several hours later. Organ dissection from the abdominal and thoracic cavities of *p63*-deficient newborn mice showed no deviation from the usual *situs* arrangement or any gross malformation, and histological sections of the viscera and brain revealed no microscopic abnormality. Water-loss assays, an *in vivo* measure of the functional permeability of the skin, revealed that *p63*-deficient animals lose approximately thirty times more water than their wild-type littermates (data not shown). It is likely that these p63-deficient animals die from dehydration.

p63-deficient newborns display striking limb defects. The forelimbs were truncated and hindlimbs were completely absent in all of the *p63*-homozygous mutant animals that were analysed visually at birth ($n = 77$). Analysis of skeletons stained for bone and cartilage indicates that the forelimbs of *p63*-homozygous mutant animals are truncated and that the distal skeletal elements are absent (Fig. 2b and c). Phalanges and carpals were absent in all of the *p63*-homozygous mutant forelimb skeletal preparations analysed, whereas more proximal forelimb structures were slightly heterogeneous in the extent of the truncation. For example, the radius was not present in any of the mutant limbs analysed, but the ulna was present in a subset (37.5%) of the limbs. Although the humerus was present in each of the mutant limbs, it was usually truncated, deformed, and smaller in girth than those of wild-type and heterozygous siblings (Fig. 2c). The femur and all distal skeletal elements were absent in all of the *p63*-homozygous mutant limbs examined (Fig. 2b, d). The hip girdle was present but lacked the ossification centre found in the wild-type sibling. Teeth are also absent in p63-deficient newborn mice (Fig. 2e).

During embryogenesis, the apical ectodermal ridge (AER), a structure required for limb outgrowth along the proximal–distal axis, can be seen in the scanning electron micrograph at the junction